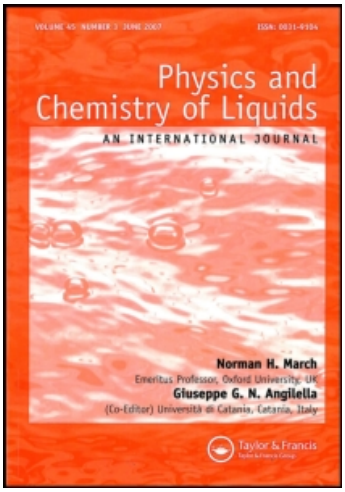

Physics and Chemistry of Liquids
Publication details, including instructions for authors and subscription information:
http://www.informaworld.com/smpp/title~content=t713646857

Study of a critical ternary microemulsion by permittivity and Kerr-effect techniques

P. Sorichetti[a]; E. Acosta[a]; D. Kurlat[a]
[a] Facultad de Ingenieria, Departamento de Fisica, Laboratorio de Sistemas Líquidos, UBA, Paseo Colon 850, Buenos Aires, Argentina

To cite this Article Sorichetti, P. , Acosta, E. and Kurlat, D.(2008) 'Study of a critical ternary microemulsion by permittivity and Kerr-effect techniques', Physics and Chemistry of Liquids, 46: 1, 59 — 70
To link to this Article: DOI: 10.1080/00319100701488490
URL: http://dx.doi.org/10.1080/00319100701488490

Physics and Chemistry of Liquids
Vol. 46, No. 1, February 2008, 59–70

Taylor & Francis
Taylor & Francis Group

Study of a critical ternary microemulsion by permittivity and Kerr-effect techniques

P. SORICHETTI*, E. ACOSTA and D. KURLAT

Facultad de Ingenieria, Departamento de Fisica, Laboratorio de Sistemas Líquidos, UBA, Paseo Colon 850, Buenos Aires, Argentina

(*Received 5 May 2007; in final form 4 June 2007*)

A critical microemulsion (AOT/decane/water, $W_0 = 34.6$ and $\phi_g = 0.068$) was studied using complex permittivity and Kerr-effect techniques. Permittivity measurements were made in the range from 150 Hz to 1.5 MHz using a circuit of a novel design. Below 100 kHz a dielectric relaxation process appears, it can be related to a Maxwell–Wagner polarization effect. Moreover, the conductivity has a clearly critical behavior in agreement with references in the literature. On the other hand, measurements of static and dynamic electric birefringence near to the critical temperature show a diverging Kerr constant and a strong asymmetry between a rise and decay of birefringence, similar to those described by Degiorgio and Piazza for similar systems [V. Degiorgio, R. Piazza. *Phys. Rev. Lett*., **55**(3), 288 (1985)]. Results are explained by assuming that the microdroplets do not change their shape but form clusters near the critical temperature. The critical exponents agree quite well with the information found in the literature for similar systems [Letamendia, E. Pru-Lestret, P. Panizza, J. Rouch, F. Sciortino, P. Tartaglia, C. Hashimoto, H. Ushiki, D. Risso. *Physica A*, **300**, 53 (2001)].

Keywords: Critical microemulsions; Electric birefringence; Dielectric spectroscopy

1. Introduction

The study of critical phenomena in soft matter systems presents very interesting aspects. The so called ''critical divergences'' are observed in many different physical processes as conductivity, light-scattering, heath capacity, sound attenuation electric conductivity and permittivity. It is the existence of large density fluctuations when approaching to the critical points (either in temperature or in concentration) could explain the great increase in relevant physical magnitudes that describe the process in spite of the essential physical differences between these phenomena. This general behavior may be described by means of exponential scaling laws.

The exponents are called ''universal'' since they show no system dependence, whereas the amplitudes are characteristic of each particular physical system. As a matter of fact,

*Corresponding author. Email: psorich@fi.uba.ar

ISSN 0031-9104 print/ISSN 1029-0451 online © 2008 Taylor & Francis
DOI: 10.1080/00319100701488490

exponents are not strictly independent between each other. They can be classified in different groups because it is possible to relate them by thermodynamic and scale arguments. Also, it is possible to associate critical amplitudes to universal relationships by similar theoretical arguments.

Electrical and electro-optical techniques have proved to be very useful tools to investigate complex fluids. In this article we present the results that were obtained by using electric induced birefringence (Kerr-effect) and electrical conductivity and permittivity determinations in a ternary microemulsion, close to a critical temperature.

The broad frequency range covered by the measurements presented in this work (150 Hz to 1.5 MHz) makes it possible to study the relaxation process related to the Maxwell–Wagner interfacial polarization of the microdroplets. This provides complementary information on the shape of the micelles as the system approaches the critical temperature in addition to neutron- and light-scattering experiments [3]. Therefore, dielectric results complement Kerr-effect measurements, which are sensitive to droplet clustering. This combination of dielectric spectroscopy and Kerr-effect techniques (in addition to light-scattering) is interesting for its application to biological systems, which usually cannot tolerate neutron irradiation. Therefore, validation with a reasonably well-known system such as the one described in this work, lends confidence to its application to less well-known systems where it is not possible (or desirable) to make neutron-scattering studies.

We have chosen to study a microemulsion W/O which it is known to have a critical behavior [4]. Critical exponents values were verified by Toprakcioglu *et al.* [5]. Nanodroplets structures at this composition have been studied. They have a 100 nm radius and are strongly polydisperse. The estimated polydispersivity is 20% [6].

Some low-frequency (below 1 MHz) complex permittivity results in similar critical systems have been reported, mainly in connection with conductivity studies of percolation processes [7,8]. Also, light-scattering experiments were carried out by several authors [9,10].

Some studies of the Kerr constant in these systems were reported by Edwards *et al.* [11] as a function of the water/surfactant concentration rate at temperatures far from the critical one. These authors show that the Kerr constant depends on the interaction between droplets.

Besides it was proved that this interaction is between aggregates. Rouven *et al.* [12] have shown that for these systems and for temperatures far from the critical the birefringence depends on nanodroplets concentration.

There are some studies on Kerr-effect in microemulsions near a transition from 1 and 2 phases. Degiorgio and Piazza [13] found that the Kerr constant does not diverge when a phase transition is reached. It rises considerably at a critical region the corresponding exponents are not well established.

2. Materials and methods

2.1. *Materials*

We have investigated a three-component microemulsion of AOT (SIGMA, without additional purification), water (previously filtered and deionized) and decane (FLUKA).

The water/surfactant molar relation (W_0) was 34.6 and the nanodroplets volume fraction (ϕ_g) was 0.068. The microemulsion mass composition (in g) was: water 2.331, decane 36.072, and AOT 1.662. ϕ_g was calculated from the concentrations (in mass) of each component.

2.2. *Methods*

2.2.1. Kerr-effect. The experimental setup was described in precedent articles [14].

The basic electric birefringence setup is shown in figure 1. Hence we shall give a short account of it. A laser beam ($\lambda = 632.8$ nm) is polarized by means of a Glen–Thomson type polarizer (''polarizer'').The beam passes through an optical cuvette (Hellma QS 500, 50 mm in length) where the liquid sample is placed. Inside the cuvette there are two stainless steel plates (Kerr cell electrodes) separated by a 2.0 mm distance. Both electrodes are connected to a pulsed high voltage source ($0 < V < 2.5$ kV).The electric source rise time is less than 100 ns. It is the application of this short pulse (E) which introduces an anisotropy in the liquid and generates the birefringence in the liquid. On leaving the Kerr cell the laser beam goes through a second polarizer (''analyzer''). Optical axes of polarizer and analyzer are at 45 and 145°, respectively, from the electric field direction in order to measure the Kerr constant sign, a quarter wave plate is placed between cuvette and analyzer. The measured light intensity is related to the difference by:

$$\Delta n = n_p - n_t = \lambda B E^2 \tag{1}$$

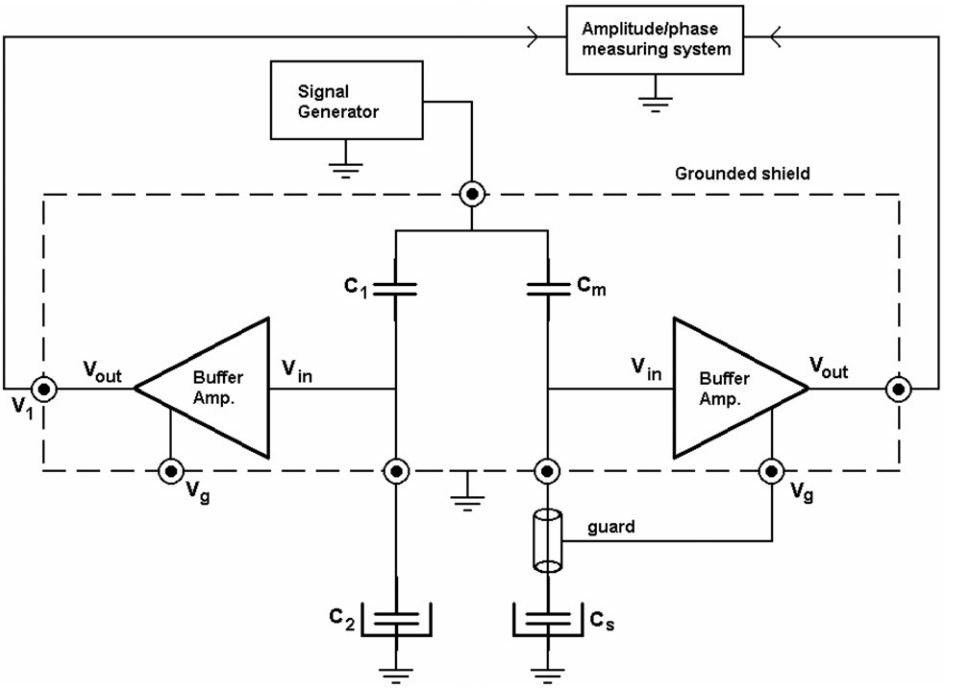

Figure 1. Measuring circuit.

n_p and n_t are parallel and perpendicular refraction indices with respect to E, respectively. The constant B is called the Kerr constant. The maximum field strength was $10^5\,V\,m^{-1}$.

The Kerr cell is full immersed on metal jacket thermalized by circulated water. A Lauda thermostat is used to temperature regulator. An independent sensor (PT100 thermoresistor) is used to measure the cell temperature. All the experiment was performed under thermalization condition of at least 2 h.

The rise and decay birefringence times processes are characterized by the following expressions respectively [15]:

$$\tau_r = \int_0^\infty \left(1 - \frac{\Delta n(t)}{\Delta n_s}\right) dt \quad \text{(rise)} \tag{2a}$$

$$\tau_d = \int_0^\infty \frac{\Delta n(t)}{\Delta n_s}\, dt \quad \text{(decay)} \tag{2b}$$

where $\Delta n(t)$ is the birefringence signal and Δn_s is the stationary value with field.

2.2.2. Permittivity and conductivity. High-frequency dielectric properties of complex fluids and biological systems (above 10 MHz) are often measured by time- or frequency-domain (TDR/FDR) reflectometry techniques, using coaxial sample cells. It implies that one of the sample electrodes must be at ground potential. However, low-frequency techniques usually require that both sample electrodes be connected to nodes different than system ground, thus making necessary to use different sample cells to make broadband dielectric measurements. This is not convenient for studies of phase transitions and critical phenomena in complex fluids, since of measurements must be made under strictly controlled conditions.

In contrast, the dielectric interface used in this work is compatible with standard coaxial sample cells used for TDR and FDR high-frequency measurements. The replacement of the reflectometer by the new interface can be easily done during the course of an experiment. Therefore, low-frequency dielectric measurements can be made without removing the sample from the high-frequency cell, avoiding any disturbance to the fluid.

The special circuit used in this work[1] was designed to make dielectric values measurements in a broad frequency range (from 30 Hz to 15 MHz) with one of the sample electrodes grounded.

The measurement circuit is shown in figure 1. Capacitors C_1 and C_2 values are precisely known and are independent of the frequency, with negligible losses. The V_G generator excites the dielectric interface with a harmonic signal of angular frequency ω. Complex amplitudes of the reference signal, $V_2(\omega)$ and measurement signal, $V_1(\omega)$, are determined without perturbing the circuit.

The sample, located in a in a high-frequency cell, is the unknown capacity C_s. Hence:

$$C_s(\omega) = C_m[k\alpha(\omega) - 1] \tag{3}$$

k is defined as:

$$k = 1 + \frac{C_2}{C_1} \tag{4}$$

and α is the ratio between the complex amplitudes of $V_2(\omega)$ and $V_1(\omega)$:

$$\alpha = \frac{V_2(\omega)}{V_1(\omega)}. \tag{5}$$

An appropriate choice of the k factor (i.e. by modifying C_2) makes it possible to keep a value into an adequate range in order to achieve a satisfactory accuracy in the amplitude and phase determinations.

A synthesized signal generator (INSTEK GW-830) and a digital oscilloscope (TEKTRONIX TDS 210) both controlled by a personal computer, they were used for excitation and signal capture. Further details on the measurement technique shall appear in [16].

3. Experimental results

Critical temperature (T_C) was 305 K approximately. It was determinate by visual inspection in sealed tubes.

At temperatures $T > T_C$ the liquid system is composed by two W/O microemulsion phases whereas below the T_C there is a W/O microemulsion single phase.

3.1. *Kerr-effect*

For $T > T_C$ the Kerr measurements were performed in the lower phase. We have limited our determinations to low voltages in order to avoid the merging of the nanodroplets. The Kerr law is valid in all the measurement range and B values are always positive.

In all the cases the rise and decay birefringence curves cannot be described by adding two or three monoexponentials. The experimental data were fitted by assuming a deformed exponential functional dependence. This behavior is very common when the system is polydisperse. The functions used to adjust the experimental data were:

$$\Delta n_r(t) = \Delta n_s\left(1 - \exp\left(-\left(\frac{t}{\varsigma_r}\right)^{\alpha_r}\right)\right) \quad \text{(rise)} \tag{6a}$$

$$\Delta n_d(t) = \Delta n_s \exp\left(-\left(\frac{t}{\varsigma_d}\right)^{\alpha_d}\right) \quad \text{(decay)} \tag{6b}$$

ζ_r and ζ_d are the characteristic times and α_r and α_d are coefficients which indicate the polydispersivity degree of the system ($0 < \alpha < 1$ and $\alpha = 1$ value indicates monodispersivity) or each one applied tension, birefringence establishment and relaxation were adjusted simultaneously and a set of Δn_s, ζ_r, ζ_d, α_r and α_d were obtained by employing equation (1). B value is determined for each temperature and with equations (2a) and (2b) characteristic times τ_r and τ_d are calculated.

In figure 2, Kerr constant data is shown as a function of temperature. The Kerr constant grows rapidly when the temperature is close to the critical value.

Characteristic times ζ_r and ζ_d represent relaxation times of the basic structures which contributes to the birefringence of the microemulsion. In figure 3, it can be appreciated that there are no significative influences between establishment and relaxation regimes.

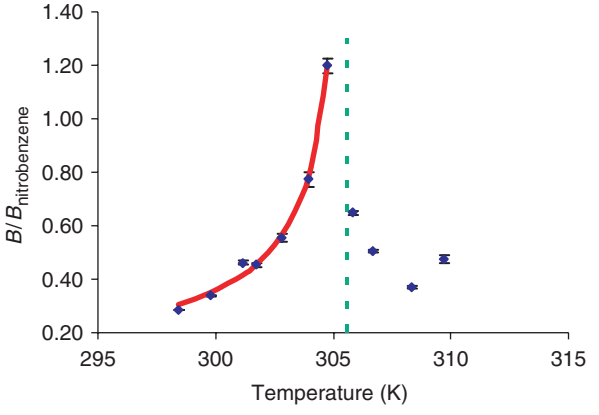

Figure 2. $B/B_{\text{nitrobenzene}}$ as a function of temperature. Continuous line represents a fitting when equation (7) is employed. $B_0 = 0.026$.

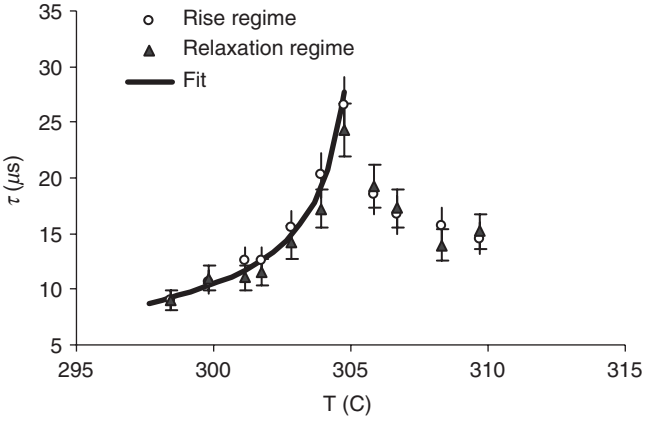

Figure 3. Characteristics times as a function of temperature.

As it is shown in figure 4, α coefficients change when establishment and relaxation regimes are taken into consideration. Now, it is not observed a dependence value for a regime (establishment or relaxation) when a temperature is fixed. Hence there is no dependence of the applied field. These results are obtained like a mean value over all applied tensions. On the other hand, the α_r and α_d dependence with temperature is similar. When E is applied, it appears a dipole–dipole interaction between nanodroplets which produces a rise in the relaxation time.

3.2. *Permittivity and conductivity of the microemulsion*

3.2.1. Real part. In figure 5, experimental results of the real part of permittivity (ε') are shown.

The frequency range was between 150 Hz and 1.5 MHz.

Measurements were taken at five frequencies in each decade of the indicated range five. Experimental values have been obtained at temperatures of 303.0, 305.5,

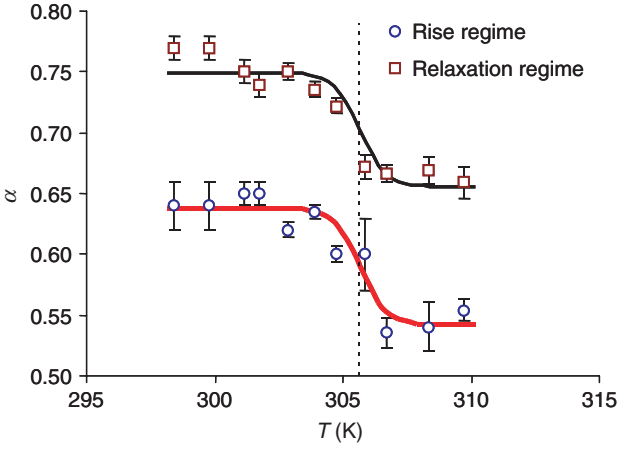

Figure 4. α coefficients.

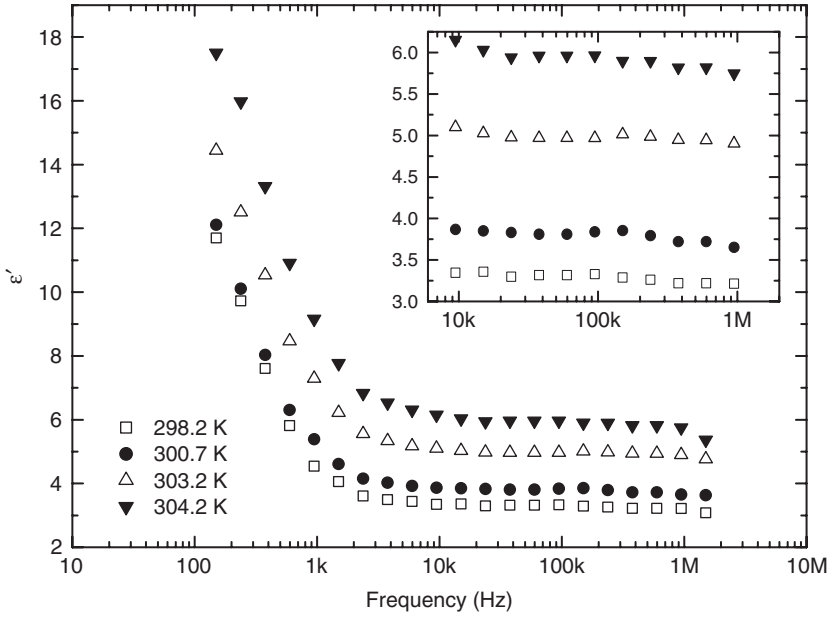

Figure 5. Real part of permittivity. The inset shows a zoom-in view for frequencies above 10 kHz.

308.0 and 309.0 K. Experimental results are the average of five different measurements at each frequency. It can be observed that the real part shows a clearly decreasing behavior up to frequencies of the order of 10 kHz. Starting approximately from this value a plateau appears. This process can be clearly appreciated in the inset in figure 5, which shows results in the 10 kHz to 1 MHz range. The behavior is qualitatively similar at all the measurement temperatures. When temperature approaches the critical value, there is a displacement towards higher permittivity.

3.2.2. Imaginary part. Experimental values of the imaginary part of the complex permittivity (ε'') are shown in figure 6. These values include the conductivity term. Experimental conditions are the same as those described in the previous paragraph.

It can be seen that ε'' presents a clearly decreasing behavior, from higher values at low frequencies to very small ones at high frequencies. When the critical temperature is approached, the low-frequency values increase significantly. The inset in figure 6 shows the imaginary part of the complex permittivity within the range from 10 kHz to 1 MHz in more detail.

4. Discussion and conclusions

4.1. *Kerr-effect*

In the study of critical phenomena, the dependence of physical variables, X, is usually modeled by a power law as a function of the reduced temperature Θ:

$$X(\Theta) = C\Theta^{\delta} \tag{7}$$

where δ is the critical exponent and C the prefactor associated to the variable X.

The reduced temperature Θ is defined in terms of the temperature T and the critical temperature T_C as:

$$\Theta = 1 - \frac{T}{T_C}. \tag{8}$$

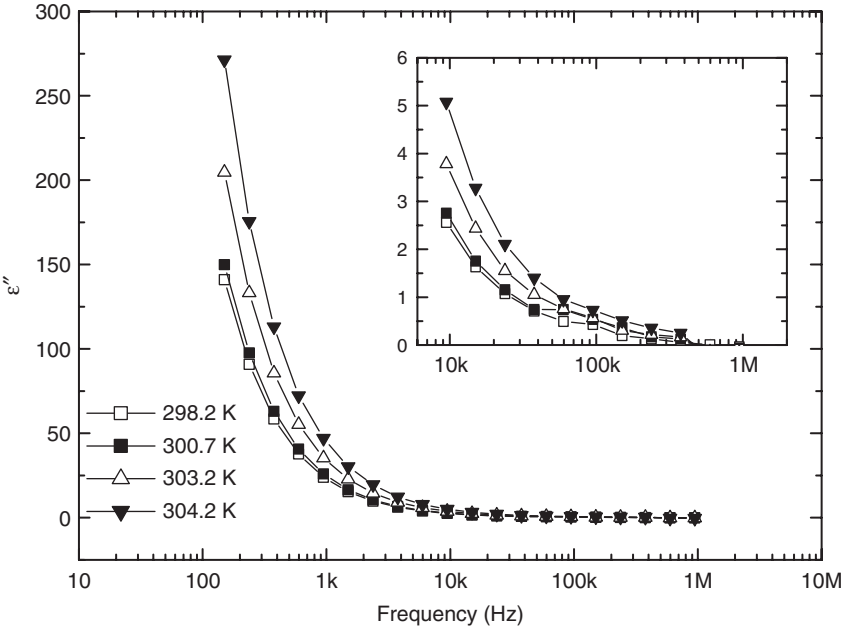

Figure 6. Imaginary part of permittivity. The inset shows a zoom-in view for frequencies above 10 kHz. Lines are a guide for the eyes.

We have employed equations (7) and (8) to fit the Kerr constant, establishment and relaxation experimental data. Results are presented in table 1. It can be seen that there are no significative differences for each T_C obtained by using each couple of data.

The exponent δ value (obtained from B) is similar to Degiorgio and Piazza [1] results.

The α values can be represented by the following expression (step pulse type)

$$\alpha_x = \Delta\alpha_x \frac{(1 - \tanh(T - T_{C,x}))}{2} + \alpha_{0,x} \tag{9}$$

with $\Delta\alpha_r = 0.096 \pm 0.011$; $\Delta\alpha_d = 0.094 \pm 0.012$; $\alpha_{0,r} = 0.54 \pm 0.01$; $\alpha_{0,r} = 0.65 \pm 0.02$ and $T_{C,r} = T_{C,d} = 32.5 \pm 0.3°C$.

This result shows that the polydispersion of the microemulsion is practically independent of the temperature up to 2°K near T_C. From temperatures greater than T_C, results show the polydispersion of the lower phase.

4.2. *Permittivity and conductivity*

For each temperature, the frequency dependence of the relative complex permittivity (ε_r) is expressed as the sum of a polarization component ($\varepsilon' - i\varepsilon''$) plus a conductivity term (σ_0/ω). In consequence, results for the imaginary part of the complex permittivity were expressed as:

$$\varepsilon''_r(\omega) = \varepsilon''_{pol}(\omega) + \frac{\sigma_0}{(\omega\varepsilon_0)}. \tag{10}$$

The first term $\varepsilon''_{pol}(\omega)$ is related to polarization relaxation (and therefore vanishes in the limit $\omega \to 0$), whereas the charge transport term $\sigma_0/(\omega\varepsilon_0)$ originates a finite conductance at $\omega = 0$. In consequence, the complex relative permittivity is given by:

$$\varepsilon_r(\omega) = \varepsilon'_r(\omega) - i\varepsilon''_{pol}(\omega) - i\frac{\sigma_0}{(\omega\varepsilon_0)}. \tag{11}$$

Furthermore, the polarization term $\varepsilon''_{pol}(\omega)$ for frequencies below 100 kHz was related to the real part $e'(w)$ according to the widely used Havriliak–Negami (H–N) dielectric function [3]:

$$\varepsilon'_r(\omega) - i\varepsilon''_{pol}(\omega) = \varepsilon_{HF} + \frac{\varepsilon_{LF} - \varepsilon_{HF}}{[1 + (i\omega\tau_0)^\alpha]^\beta}. \tag{12}$$

In this function, ε_{LF} represents the asymptotic low-frequency limit of the relative permittivity and ε_{HF} indicates the limiting value at high frequencies. It is assumed that only one relaxation process takes place within the frequency range of the fitting. The relaxation strength of the process $\Delta\varepsilon$ is defined as the difference between the

Table 1. Critical coefficients and prefactors for electric birefringence fitted from experimental data.

Data	C	δ	T_C (K)
$B/B_{nitrobenzene}$	0.026 ± 0.010	0.65 ± 0.10	305.6 ± 0.3
ζ (μs)	1.46 ± 0.58	0.49 ± 0.10	305.6 ± 0.4

asymptotic low-frequency and high-frequency values, $\Delta\varepsilon = \varepsilon_{LF} - \varepsilon_{HF}$, and τ_0 is the relaxation time. It may be seen similar to the Debye process (which corresponds to $\alpha = \beta = 1$), the polarization loss $\varepsilon''_{pol}(\omega)$ has a broad peak ("relaxation peak") centered at $1/\tau_0$. The α parameter ($0 < \alpha < 1$) represents a symmetrical broadening of the relaxation peak in comparison with the Debye process, whereas the β parameter ($0 < \beta < 1$) models an unsymmetrical broadening. The first case ($\alpha = 1, \beta < 1$) corresponds to a Cole–Cole process, and the second ($\alpha = 1, \beta < 1$) represents a Davidson–Cole relaxation. It must be remarked that when $\beta < 1$ the angular frequency of relaxation peak is shifted from its value for the Debye process $1/\tau_0$ due to the unsymmetrical broadening.

From the dependence of the parameters of the H–N function with temperature, the behavior of the Maxwell interfacial polarization near the critical temperature may be studied, since its frequency range is well within the 100 kHz range. It is easy to see that the ε_{HF} value corresponds to the plateau observed in the inset of figure 5 between 10 and 100 kHz. The parameter values fitted to equations (11) and (12) are given in table 2. It may be seen that the process corresponds to a Cole–Cole model ($\alpha \approx 0.9, \beta < 1$). This broadening with respect to a Debye process is consistent with the superposition of relaxation times due to system polydispersity, as revealed by Kerr-effects results.

The dependence of σ_0, ε_{HF}, and $\Delta\varepsilon$ with reduced temperature, Θ, was fitted according to equation (7). The values of the critical exponent δ, the prefactor C and the critical temperature T_C for the conductivity σ_0, the high-frequency asymptotic permittivity ε_{HF} and the relaxation strength $\Delta\varepsilon$, together with the root-mean-square error for the fitting, are given in table 3.

It may be seen that critical temperature agrees well with the value of 305 K determined by visual inspection. The conductivity σ_0 shows a clearly critical behavior, attributable to the well-known percolation process [8].

From tables 2 and 3 it is easy to see that the dielectric relaxation time τ_0 and the relaxation intensity $\Delta\varepsilon$ practically are independent of temperature. If this relaxation

Table 2. Fitted values of the parameters of complex permittivity, equations (11) and (12).

T (K)	298.2	300.7	303.2	304.2
σ_0	1.12E-06	1.22E-06	1.70E-06	2.23E-06
ε_{LF}	14.19	15.34	16.85	19.75
ε_{HF}	3.31	3.85	4.94	5.94
τ_0(s)	5.42E-04	5.94E-04	5.19E-04	3.95E-04
α	0.94	0.93	0.88	0.89
β	1	1	1	1
$\Delta\varepsilon$	10.88	11.49	11.91	13.81

Table 3. Critical coefficients and prefactors for the parameters of complex permittivity.

	δ	C	T_C	RMS error
σ_0	0.31	3.4E-07	304.8	3E-08
ε_{HF}	0.37	0.85	305.7	0.01
$\Delta\varepsilon$	0.08	7.99	304.5	0.22

process is analyzed in terms of the Maxwell–Wagner–Sillars model [3] these results may be explained considering that micelles shape do not change appreciably when the critical temperature is approached.

According to this model, the relaxation time of the polarization is given by

$$\tau_k = \frac{c_k}{d_k} \tag{13}$$

where $c_k = \sigma_a + (\sigma_p - \sigma_a)L_k$, $d_k = \varepsilon_0[\varepsilon_a + (\varepsilon_p - \varepsilon_a)L_k]$ where σ_a, ε_a, σ_p and ε_p are the conductivity and permittivity of the dispersed and continuous phases, respectively, and L_k is the shape factors that depend on the micelles geometrical form. Also, the relaxation strength is dependent on the shape factors L_k [3].

In the narrow temperature range studied in this work, σ_a, ε_a, σ_p and ε_p are almost constant. Therefore, since experimental results indicate that τ_0 and $\Delta\varepsilon$ do not change, it follows that the shape factors L_k remain unchanged. In consequence, even near the critical temperature the assumed spherical shape of the microdroplets is not modified.

4.3. *Conclusion*

In summary, low-frequency dielectric and Kerr-effect measurements provide complementary results. From the results of other experimental techniques, light and neutron-scattering [10], and the Kerr-effect measurements presented in this work, it may be assumed that the correlation between droplets increases considerably near T_C (''clustering''). Letamendia *et al.* [2] have studied sound speed, sound attenuation, and dielectric properties of a similar system ($W_0 = 40.8$, $\phi_g = 0.1$, with $T_C = 40^\circ C$). Results of dielectric measurements between 10 MHz and 10 GHz are also given in [2]. The low-frequency limiting (''static'') value of permittivity given by Letamendia *et al.* corresponds to the high-frequency asymptotic value (ε_{HF}) in this work. Their ''static'' permittivity value shows a critical behavior with $\delta = (0.37 \pm 0.05)$, which is in good agreement with the result in table 3. In the high RF range (200–800 MHz) they found a relaxation process where the relaxation time and intensity have a critical dependence with temperature near T_C. This result is explained by the fractal clustering of the microdroplets, in agreement with the interpretation of Kerr-effect results in this work.

Dielectric measurements in this work are complementary with the high-frequency range studied by Letamendia *et al.* Low-frequency results show that the individual microdroplets maintain their shape, but are not able to reveal the clustering between them.

References

[1] V. Degiorgio, R. Piazza. *Phys. Rev. Lett.*, **55**(3), 288 (1985).
[2] L. Letamendia, E. Pru-Lestret, P. Panizza, J. Rouch, F. Sciortino, P. Tartaglia, C. Hashimoto, H. Ushiki, D. Russo. *Physica A*, **300**, 53 (2001).
[3] K. Asami. *Prog. Polymer Sci.*, **27**, 1617 (2002).
[4] J.S. Huang, M.W. Kim. *Phys. Rev. Lett.*, **47**(20), 1462 (1981).

[5] C. Toprakcioglu, J.C. Dore, B.H. Robinson, A. Hawe, P. Chieux. *J. Chem. Soc., Faraday Trans. I*, **80**, 413 (1984).
[6] M. Zulauf, H.-F. Eicke. *J. Phys. Chem.*, **83**(4), 480 (1979).
[7] S. Bhattacharya, J.P. Stokes, M.W. Kim, J.S. Huang. *Phys. Rev. Lett.*, **55**(18), 1184 (1985).
[8] C. Robertus, J.G.H. Jooosten, Y.K. Levine. *J. Chem. Phys.*, **93**(10), 7293 (1990).
[9] P. Codastefano, F. Sciortino, P. Tartaglia, F. Bordi, A. Di Biadio. *Colloids Surf. A*, **140**, 269 (1998).
[10] L. Vicari. *J. Appl. Phys.*, **88**(1), 7 (2000).
[11] M.E. Edwards, X.L. Xu, J.-S. Huang, H. Kellay. *Phys. Rev. E.*, **57**(1), 797 (1998).
[12] J. Rouven, J.-M. Couret, M. Lindheimer, J.-L. Dejardin, P. Marrony. *J. Chimie Physique*, **76**(3), 289 (1979).
[13] V. Degiorgio, R. Piazza. *Prog. Colloid Polymer Sci.*, **73**, 1184 (1987).
[14] D.H. Kurlat, M. Bisceglia, E. Acosta, B. Ginzberg. *Colloids Surf. A*, **108**, 137 (1996).
[15] S.P. Stoylov. *Colloid Electro-Optics: Theory, Techniques, Applications*, Academic Press, London (1991).
[16] P.A. Sorichetti, C.L. Matteo. *Measurement*, **40**, 437 (2007).